53-90
[redacted]

OBSERVATIONS OF PLASMA DYNAMICS IN THE COMA OF P/HALLEY BY THE GIOTTO ION MASS SPECTROMETER

P- 23

117929

N93-13468

B. E. Goldstein, R. Goldstein, M. Neugebauer

Jet Propulsion Laboratory
4800 Oak Grove Drive
Pasadena, CA 91109 USA

S. A. Fuselier, E. G. Shelley

Lockheed Palo Alto Research Laboratory

H. Balsiger

University of Bern

G. Kettmann, W.-H. Ip, H. Rosenbauer, R. Schwenn

Max-Planck Institut für Aeronomie

Submitted to Journal of Geophysical Research
December 26, 1990

ABSTRACT

Observations in the coma of P/Halley by the Giotto Ion Mass Spectrometer (IMS) are reported. The High Energy Range Spectrometer (HERS) of the IMS obtained measurements of protons and alpha particles from the far upstream region to the near ionopause region, and of ions from mass 12 to 32 at distances of about 250,000 km to 40,000 km from the nucleus. Plasma parameters from the High Intensity Spectrometer (HIS) of the IMS obtained between 150,000 to 5000 km from the nucleus are also be discussed. The distribution functions of water group ions (water group will be used to refer to ions of 16 to 18 m/q, where m is in AMU and q is in unit charges) are observed to be spherically symmetric in velocity space, indicating strong pitch angle scattering. The discontinuity known as the magnetic pile-up boundary (MPB) is apparent only in proton, alpha, and magnetometer data, indicating that it is a tangential discontinuity of solar wind origin. HERS observations show no significant change in the properties of the heavy ions across the MPB. A comparison of the observations to an MHD model (Wegmann *et al.*, 1987) is made. The plasma flow directions at all distances greater than 30,000 km from the nucleus are in agreement with MHD calculations. However, despite the agreement in flow direction, within 200,000 km of the nucleus the magnitude of the velocity is lower than predicted by the MHD model and the density is much larger (a factor of 4). Within 30,000 km of the nucleus there are large theoretical differences between the MHD model flow calculations for the plane containing the magnetic field and for the plane perpendicular to the magnetic field. The observations agreed much better with the pattern calculated for the plane perpendicular to the magnetic field. The data obtained by the High Energy Range Spectrometer (HERS) of the IMS that are published herein have also been provided to the International Halley Watch archive.

INTRODUCTION

The Giotto spacecraft of the European Space Agency approached Halley's comet at a speed of 68.4 km/sec, with an angle between the spacecraft velocity in the comet frame and the sun-comet line of 107°, and with closest approach occurring at 00:03 UT on March 14, 1986. Among the investigations on the spacecraft was the Ion Mass Spectrometer (IMS). The major focus of this paper is the presentation of heavy ion plasma parameters and particle distributions obtained by the HERS. Also presented are improved estimates of proton and alpha particle parameters obtained by the HERS. The proton, alpha particle, and heavy ion observations are also compared to the predictions of an MHD model. Recent compositional results of data from the High Energy Range Spectrometer (HERS) of the IMS (Neugebauer *et al.*, 1990) have recently been accepted for publication.

DESCRIPTION OF INSTRUMENT AND METHOD OF ANALYSIS

The HERS measured positive ions for energies up to about 4 keV, depending on the mass being observed and the view direction. The instrument had a fan-like field of view that rotated about the spin axis; the inner edge (the edge towards the comet direction) of the fan was 15° from the spin axis, while the outer edge was 75° from the spin axis. The instrument had 4 modes (proton, light, medium, and heavy); each mode was measured once every 4 spins, so that measurements of different species were obtained at 16 second intervals. The HERS sensor had energy windows that were of constant width in momentum per unit charge (rather than constant width in the logarithm of energy per unit charge as for a conventional electrostatic analyzer). Further description of the experiment is provided in Balsiger *et al.* (1986a); first results are reported in Balsiger *et al.* (1986b).

A number of different methods have been used to analyze Giotto HERS data. The consequence of constant momentum width windows is that, although good energy resolution is obtained for heavy ions, the energy window for alpha particles is 64 eV full width at half maximum, and for protons is twice as wide. Two problems result if a straightforward moment analysis is used: 1) the thermal broadening along the line of sight is overestimated, and 2) for low proton and alpha particle velocities, the bulk flow speed is overestimated due to the low energy cutoff (10 eV) of the instrument not being properly taken into account. Additionally, there is a cone of 15° half-angle centered on the cometary direction in which the HERS sensor does not obtain measurements. Goldstein *et al.* (1987, Figs. 1 and 3) used fits to a Maxwell-Boltzmann distribution integrated over the instrument response to estimate proton and alpha velocities, whereas the heavy ion velocities were calculated from a moment technique. Since that time, we have recalibrated the proton mode of the flight spare, and obtained an improved understanding of the instrument response to low energy protons. In the present paper, we obtain estimates of plasma parameters by assuming that distributions are spherically symmetric in velocity space. The density in a shell is then computed by averaging over the observations within the shell. The velocity of the distribution (i.e., center of the shells) is adjusted using an iterative least squares technique to reduce the error in a fitting parameter. This fitting parameter is the first moment of the distribution obtained by integrating over the instrument field of view, and it is compared to the first moment obtained by integrating the assumed distribution over the instrument field of view. This procedure corrects for errors if a portion of a spherical shell is out of the field of view; however, it can not compensate for an entire shell being out of the field of view. This happens in the cold, dense region of the inner coma when the bulk velocity relative to the spacecraft is nearly from the ram direction. In Figure 1 we have plotted the velocity of water group ions in instrument coordinates obtained by the HERS sensor as estimated from model fits to the HERS data. The datum points represent data averaged over time periods ranging from approximately two minutes when close to the comet to eight minutes when far from the comet. The measurements obtained by the HERS sensor should include all velocity shells up until about 23:38 (102,000 km from the comet), after this time it can not be said with complete assurance that none of the cold plasma has been missed because the estimated velocities fall very close to the boundary of the 15° half-angle cone. When the center of the distribution falls well within the 15° half-angle cone (i.e., the last four points starting at 23:44:51 UT, within 75,000 km of the nucleus), then the cold core of the distribution is definitely not seen by the HERS sensor. The estimate of plasma direction may also be verified by comparison to data from the High Intensity Spectrometer (HIS) of the IMS (see Fig. 6 below). Improved density and compositional measurements obtained by the HERS experiment have recently been submitted for publication

(Neugebauer *et al.*, 1990); similar field of view effects apply to these densities and abundances as well. The data obtained by the High Energy Range Spectrometer (HERS) of the IMS that are published herein have also been provided to the International Halley Watch archive.

REVISED PROTON AND ALPHA PARTICLE MEASUREMENTS

The general features of the outer cometosheath have been described by Balsiger *et al.* (1986), Neubauer *et al.* (1986), Johnstone *et al.* (1986), Goldstein *et al.* (1987), Glassmeier *et al.* (1987), Rème *et al.* (1987), and others. In particular, Goldstein *et al.* (1987) have published earlier HERS alpha particle analyses, and HERS parameters for all species including protons have been submitted to the National Space Science Data Center. Our newly reduced proton and alpha particle measurements using the revised techniques just discussed in this paper have been submitted to the NSSDC and the International Halley Watch archives. We publish these revised estimates herein. Due to the upper energy limit of the HERS sensor, and counting statistics, only H^+, m/q=2, and m/q=4 observations were obtained at distances greater than 250,000 km. The m/q=2 particles are either He^{++} or H_2^+, and the m/q=4 particles are He^+. Shelley *et al.* (1987) have discussed the conversion of He^{++} to He^+. Fuselier *et al.* (1988, 1990).have investigated the pick-up of H_2^+; the m/q=2 species is composed almost entirely of He^{++} until after 23:30 UT (125,000 km from the nucleus). The plasma parameters are shown in Figure 2 for the period 19:00 UT to 24:00 UT. The speed (km/sec) in a comet centered frame is shown in the upper panel, the next panel shows number density (cm^{-3}, alpha particle densities are multiplied by 10), the next shows log temperature (°K), and the lowest panel shows pressure ($dynes/cm^2$). Proton parameters are shown as solid lines, alpha particles parameters as dashed lines, and water group parameters as dotted lines. The water group temperature does not include contributions from particles in velocity shells with radii greater than 100 km/sec. It can be seen that there is excellent agreement between the proton and He^{++} speeds until about 21:45; after this time there is an increasing divergence of the estimates. As mentioned, the instrument has a rather broad energy acceptance for protons, and we interpret this difference as most likely to be due to poor velocity resolution for protons. The alpha velocity should be better determined than the proton velocity in this region.

HEAVY ION DISTRIBUTIONS

The general characteristics of heavy ion distributions should depend upon the injection of pick-up ions, their scattering in pitch angle and energy, adiabatic (de)compression as the plasma is compressed(expands) and loss by recombination or charge exchange. At distances for which HERS could obtain measurements, recombination is unimportant (Ip,1989), but the data provide support for the importance of scattering in pitch angle and loss by charge exchange. To demonstrate the importance of pitch angle scattering, we show in Figure 3 contours of common logarithm of phase space density of water group ions for a 5 minute averaging period centered at 23:27:39 UT. For this period the average location for a picked-up ring-beam distribution was at a pitch angle of 71.7° from the magnetic field direction with a velocity amplitude of 29.6 km/sec. The expected location for the pick-up beam is indicated by the cross. It can be seen that the pick-up location is within the region (dark grey) of maximum phase space density. There is also evidence for considerable scattering in pitch angle; a shell (light grey region) has been formed that includes the pick-up location. Although pitch angle scattering is clearly very important, it is not sufficiently rapid to obliterate the peak in the vicinity of the pick-up location. It can be seen that diffusion not only in pitch angle, but also in velocity, has occurred with the particles being scattered to lower velocities than the pick up velocity. Yoon (1990) and Yoon and Ziebbell (1990) have discussed mechanisms that cause diffusion in energy.

To investigate the evolution of the distribution as the comet is approached, we show the water group ion densities in two different formats. In Fig.4 are shown the phase space densities averaged over spherical velocity shells with the bottom line being the earliest data and the top line being the latest. The leftmost value plotted (smallest value of shell radius) varies from case to case because of poor counting statistics when the phase space volume of the shell is small. Comparison with the water group speed in the comet frame (vertical arrows marked on plots) shows that the peak of the distribution appears at (or just below) the local pick-up velocity. There are no observations at the last time shown (23:52 UT) for the lowest velocity shells because the cold distribution has moved into the unobserved cone in the ram direction (see Fig. 1).

At 254,000 km (23:00:30) there are higher densities in the region 50 to 60 km/sec radii than in the lower velocity shells (the apparently larger value in the 10-20 km/sec radii may be counting statistics as the volume of this portion of phase space is relatively small). The enhancement in the 50 to 60 km/sec radii region is reasonably good agreement with a pick-up velocity of 63 km/sec (plasma velocity in the comet frame) at this time; the center of the distribution (shell radii of 50 km/sec or less) has not been filled in by energy diffusion. As the comet is approached, the pick-up velocity decreases and the number of neutrals being ionized increases; for these reasons one would expect that the density in intermediate shells should increase, and then the density in the lowest velocity shells should increase later to even larger values. As expected, the peak of the distribution moves to lower velocities at later times. These changes are shown more quantitatively in Figure 5. At the highest energy shells shown (radii of 50-60 km/sec) the phase space density decreases from 23:05 to 23:14, whereas in the next highest velocity shells (radii of 40-50 km/sec) the phase space density is simultaneously increasing. The phase space densities in these shells is roughly constant from 23:10 to 23:40 (220,000 to 95,000 km), and then decreases rapidly due to charge exchange in the near vicinity of the comet (after about 23:45 UT, within 95,000 km). The other, lower velocity, shells, (with the exception of 0 to 10 km/sec) all show a pattern of increasing flux as the comet is approached, followed by a decrease during later times. The shells from 30-40 km/sec show a possible modest decrease from 23:25 to 23:40, before the precipitous decrease after 23:40 caused by charge exchange. It could be argued that a similar decrease occurs in the 40-50 km/sec shells from about 23:20 to 23:40, although the data are somewhat scattered and could equally well be argued to show no change during this period. The cause of the drop in the 30-40 km/sec shell radius region from 23:25 to 23:40 is unclear. Charge exchange might be occurring, although the neutral densities in these regions are low. Adiabatic compression due to flow deceleration would affect the distribution function, by increasing the local spatial density, but moving particles to shells with larger velocity radii. However, as the phase space density in the 20-30 km/sec region was equal to or greater than the value in the 30-40 km/sec region, the net effect of adiabatic compression would be to increase the phase space densities in the 30-40 km/sec shell region during the period 23:20 to 23:40. Diffusion in energy space would also tend to decrease phase space densities in peak regions (radii of 30 km/sec or less during this period), and increase it at greater distances. Thus, the flat behavior of the 50-60 km/sec region from 23:20 to 23:40, the decrease in the 30-40 km/sec region, and the debatable behavior in the 40-50 km/sec region may result from a balance of several processes. Detailed comparisons with theoretical models will be required to further understand these behaviors.

MAGNETIC PILE-UP BOUNDARY (MPB, OR "COMETOPAUSE")

At 135,000 km from the nucleus (23:30:00 UT), the spacecraft passed through a discontinuity designated as the magnetic pile-up boundary (Neubauer, 1987). A somewhat similar boundary observed by the plasma experiment on the VEGA spacecraft (Gringauz *et al.*, 1986) was referred to as a "cometopause" and was interpreted as a region in which a rapid build-up of cometary ions occurs. Neubauer (1987) concluded that the MPB had to be either a tangential discontinuity, or a slowly propagating rotational discontinuity with strongly differing plasma properties on either side. The plasma distribution from just before the MPB shown in Fig. 3 has no strong anisotropy; nor is there a strong anisotropy in the distribution (not shown) just after the MPB. The MPB has been of some interest because of interpretations that it might be due to a rapid charge exchange of plasma ions with neutrals with a run-away rapid growth due to deceleration of the flow by the pick-up process. Our data, however, do not show any remarkable changes in the properties of the heavy ion distributions across the pile-up boundary (Figs. 4,5), but do show a discontinuity in the properties of the protons and alpha particles (Fig.2, see also Fig. 2 of Goldstein *et al.* (1987) and Fig. 4 of Neugebauer *et al.* (1990)).

If the MPB is a tangential discontinuity, there should be no flow across it. The normal to the discontinuity is (.097, .993, -.059) in HSE coordinates (Neubauer, 1987); i.e., the normal is almost exactly in the y-direction. We compute (Table 1) the HSE velocity difference in km/sec, $\Delta V = V_{outside} - V_{inside}$, across the interface using HERS proton, alpha particle, and water group data, and HIS water group data. Also shown in Table 1 is the angle, θ, between the velocity difference and the normal to the discontinuity. If the MPB is a tangential discontinuity, then for an ideal MHD fluid ΔV_y should be zero and θ should be 90^o. Because of time variations in the data, we have taken both 2.5 and 5 minute averages on either side. Because the HERS water group parameters were not available at 2.5 minute intervals upstream of the MPB the 5 minute value upstream was used for both the 2.5 and 5 minute cases. Upstream 2.5 minute averages were not available for HERS water group data because it was necessary to have longer integration periods further from the comet, and the MPB happened to be a location where the integration period was changed in the analysis. It can be seen that the alpha particle and proton velocity differences are at a substantial angle to the normal to the discontinuity, about 65° to 70°. The fact that this angle is not 90° (as would be expected for a tangential discontinuity) might be attributable both to error in determination of the normal to the discontinuity (λ_2/λ_3 was 12.5, Neubauer, 1987), and, more likely, to errors in measurement of both proton and alpha particle velocities. The water group ΔV_z estimates from HIS and HERS disagree by about 4 km/sec; the cause of this is unknown and may reflect measurement error. The ΔV_y component (i.e., the normal component, which should be zero for a tangential discontinuity) of the alpha velocity changes in sign according to whether 2.5 or 5 minute averages are used. Both HIS and HERS find a decrease of 2.5 to 3 km/sec in the y-component of the water group velocity as the spacecraft crosses the MPB. Since the ΔV_y result does not depend upon averaging period, and both experiments agree, we believe this result is probably real, but are not absolutely certain because of the unexplained disagreement in the ΔV_z estimate.

TABLE 1

ANGLES BETWEEN COMETOPAUSE NORMALS AND VELOCITY CHANGES

	ΔV_x	ΔV_y	ΔV_z	θ
protons, 5 minute averages	7.9	3.4	-8.2	67
protons, 2.5 minute averages	9.8	3.7	-5.4	65
alphas, 5 minute averages	8.7	-9.5	-13.5	65
alphas, 2.5 minute averages	7.5	4	-14.5	71
water group, HERS, 5 minute avg.	-4.5	-2.5	3.5	60
water group, HERS, 2.5 minute avg.	-3.0	-3.0	3.0	48
water group, HIS, 5 minute avg.	-2.0	-2.8	-1.1	36
water group, HIS, 2.5 minute avg.	-2.9	-3.0	-1.0	42

The 2.5 minute averages of proton and alpha particle densities before the MPB are 5.9 cm^{-3} and 0.21 cm^{-3}, respectively, whereas after the MPB the corresponding values are 2.8 cm^{-3} and 0.13 cm^{-3}. The sharp drop in both alpha and proton densities at the MPB support Neubauer's suggestion that the MPB is a tangential discontinuity, and are inconsistent with his alternative suggestion that the MPB is a slowly propagating rotational discontinuity. The tangential discontinuity hypothesis, however, appears to be inconsistent with the marginal evidence for normal flow of water group ions across the boundary. One explanation might be

the presence of multi-fluid (proton and water group) waves as proposed by Sauer and Motschmann (1989).

We have attempted to verify the pressure balance across the tangential discontinuity. However, this requires estimating perpendicular and parallel temperatures for the water group ions; accurate values are necessary as the water group dominates the plasma pressure. Unfortunately, the variation (due to counting statistics and background) between estimates of the pressures made using different techniques is so large that it precludes an accurate estimate of the pressure change across the MPB.

COMPARISON TO MHD MODELS

Wegmann *et al.* (1987) and Schmidt and Wegmann (1990) have undertaken a numerical MHD model of the dynamical flow and chemical reactions of the plasma at Comet Halley. The dynamics are treated with a three dimensional single fluid model, while the compositional variations are computed in a two dimensional axially symmetric flow field. The Schmidt and Wegmann paper uses a grid refined by a factor of two over that used by Wegmann *et al.* , and corrects an error in the calculation of the ion temperature. A comparison between the large scale flow direction observed by the IMS and the MHD calculations of Wegmann *et al.* (1987) is shown in Fig. 6. The data are plotted in aberrated solar wind coordinates. We have defined these coordinates with the x axis pointing opposite to the direction of the upstream solar wind flow (taken to be {-365.,-17,17} km/sec in Halley solar ecliptic coordinates), with the y axis in the plane containing the spacecraft-comet velocity difference in the approximate direction of the HSE y coordinate. In these aberrated coordinates the angle between the upstream direction and the comet-spacecraft velocity difference is 103° (rather than the 107° angle between the HSE x-axis and the velocity difference), and there is a rotation of roughly 11° in the y-z plane from the HSE y-z components. The units of the axes are megameters. The spacecraft trajectory is shown as the sloping line. At large distances from the comet the best velocity measurements obtained by the experiment are given by alpha particle data; these data are plotted as vectors extending upwards from the trajectory. Closer to the comet the HERS instrument obtains water group data; these data are shown as the lines extending downwards from the trajectory. Finally, closest to the comet the best data are water group data obtained by the HIS sensor and are shown as lines extending upwards from the trajectory. The HIS velocity vectors shown are based upon the same data set described by Kettmann et al. (1990), but are rotated into aberrated coordinates (two different methods of data reduction were used by them; the data shown in Fig. 7 are that from their method of ignoring the innermost angular channel during the last ten minutes before encounter). The alpha particle data may be distinguished from the HIS data due to their separation by a gap in the upwards pointing lines. Different scales are used for plotting the alpha particle velocities and the water group velocities. The short vertical line in the lower center of the figure is the length of a 100 km/sec alpha particle vector in the plot, and is also the length of a 20 km/sec water group vector (both HIS and HERS). It can be seen that there is generally good agreement between the flow directions predicted by the model and the observations. One exception to this rule is the strong deflection observed just inside the bow shock that is not predicted by the MHD model (which does not resolve the shock well)

In Fig. 7 is shown a comparable plot of the HIS data for the region within 30,000 km of the nucleus; the units of the axes are 10^4 km and the vertical line in the lower center of the figure denotes a vector that is 10 km/sec in magnitude. The data are compared to the calculation of Wegmann *et al.* (1987) for the flow in the plane perpendicular to the magnetic field, and it can be seen that overall there is good agreement (except close to the comet). By contrast, Wegmann *et al.* (1987) have also presented the flow in the plane containing the magnetic field. In this plane the recombining plasma can flow down along field lines towards the comet, and the flow close to the comet is actually converging towards the comet rather than diverging from it. (This would be the case if the interplanetary magnetic field were in the ecliptic plane and if the comet had been approached in a trajectory lying in the ecliptic.) The Wegmann *et al.* calculations would also predict an ionopause elliptical (rather than circular) in cross-section, with the greater width in the direction not confined by draped magnetic fields. This might account for a tilt of the ionopause surface reported by Neubauer (1987, see Fig. 4). The plasma velocity observations do not agree at all (comparison not shown) with the flow pattern predicted by Wegmann *et al.* (1987) for the plane containing the magnetic field.

Which case should apply is problematic. Neubauer (1987) reports that the angle of the magnetic field out of the ecliptic plane is large and variable close to the comet. This suggests that the situation should be a compromise between the two cases reported by Wegmann *et al.* (1987); however, as mentioned earlier, the flow pattern observations agree very well with the calculation for the flow in the plane perpendicular to the magnetic field.

It may also be noted that the flow directions observed by the HIS angle analyzer within about 10,000 km of the comet do not agree with reasonable expectations. This is in part due to observational difficulties; the plasma is flowing past at 68 km/sec in the spacecraft frame and we are trying to measure a small deviation from this value. A further problem is that as the comet is approached the plasma gets colder, and eventually most of it lies in the field of view of the innermost angle analyzer. However, as the count rate became higher, some problem with this angular channel became apparent (Kettmann *et al.*, 1990), so the data that we present here are derived ignoring this channel. This means that we do not have a good measurement of the velocity component in the ram direction from HIS angle analyzer alone during the last several minutes. It is possible that recently completed reductions and analyses of the HIS mass analyzer calibrations may allow use of the mass analyzer data to resolve these ambiguities in the future.

In Fig. 8 are shown comparisons to other parameters of the MHD model of Schmidt and Wegmann (1990). The plasma parameters plotted are proton density, alpha particle velocity, water group density, velocity, and temperature as measured by the HERS, and water group velocity and temperature as measured by HIS. Comparing first the velocity prediction of the Schmidt and Wegmann paper to the alpha observations, we notice that there is excellent agreement in the outer portions of the comet (R greater than 250,000 km). At 250,000 km there is good agreement between both the prediction, the alpha particle velocity, and the water group velocities that the HERS detector observed beginning at that distance. However, at about 200,000 km a very noticeable difference has developed between the observation of the water group ions and the predictions of the model (we do not compare to the alpha velocities, which disagree with the water velocities, because the water group dominates the mass and the alpha velocity determination becomes less reliable as the comet is approached). Simultaneously, a large increase in the ion density above the values predicted by the model is observed.

It is not surprising that the model would simultaneously underestimate the density and overestimate the velocity. If too much pick-up plasma were added to the flow, conservation of momentum would require a reduction in the flow velocity. Alternatively, if for some reason the model gives too low a flow velocity, there would be greater time for addition of mass to the flow. For example, an underestimate of the neutral ionization rate might cause these disagreements. The MHD calculation assumed a single fluid, whereas the cometary plasma is composed of both solar wind protons and cometary pick-up ions. However, throughout the region where the disagreement occurs (250,000 to 25,000 km), the plasma mass density is strongly dominated by the pick-up ions, so it does not seem likely that relative velocity differences between solar wind and pick-up ions could explain the discrepancy. Temporal variation in the upstream solar wind density and velocity might also cause errors in the prediction.

Another noteworthy disagreement between the model and the observations is the apparent increase in observed HIS ion temperature above predicted values within 10,000 km of the nucleus, and below predicted values for distances between 16,000 to 250,000 km from the comet. The measured temperatures in the region close to the comet are in agreement with similar temperatures reported by Schwenn et al. (1987) from IMS-HIS mass analyzer data, and by Lämmerzahl et al. (1987) from neutral mass spectrometer data. A one dimensional MHD model of the inner coma (Cravens, 1989) does predict a region of increased temperature due to ion-neutral friction in the collisionally coupled region external to the ionopause. The region in which the temperatures measured by HERS and HIS are lower than the model (16,000 km to 250,000 km from the nucleus) can be explained by two possibilities. First, the two fluid nature of the plasma might result in some of the internal kinetic energy of the flow being maintained as a relative drift between solar wind ions and cometary ions. Although we did not regard such a two fluid effect as a likely explanation of the density/velocity discrepancy, the temperature of the plasma is much more sensitive to such effects. Second, the HERS temperatures were calculated using a cut-off for velocity shells with radii greater than 100 km/sec, and the HIS temperatures were calculated from Maxwell-Boltzmann fits to the total distribution. It is possible that there might be a hot unobserved or unmodelled shell at larger energies, and that the measured temperatures are too low. However, even at distances less than 30,000 km the disagreement is quite striking, and at such distances the mass and temperature should be dominated by the cold pick-up plasma. So, we do not believe that observational errors account for the disagreement.

ACKNOWLEDGEMENTS

The research at JPL was done under a contract between the California Institute of Technology and the National Aeronautics and Space Administration under the the sponsorship of the Magnetospheric Physics program. Research at Lockheed was supported by NASA through contract NASW-4336. The work was also supported by the Swiss National Science Foundation and the German Bundesministerium für Forschung and Technologie.

REFERENCES

Balsiger, H., K. Altwegg, F. Buehler, J. Fischer, J. Geiss, A. Meier, U. Rettenmund, H. Rosenbauer, R. Schwenn, J. Benson, P. Hemmerich, K. Sager, G. Kulzer, M. Neugebauer, B. E. Goldstein, R. Goldstein, E. G. Shelley, T. Sanders, D. Simpson, A. J. Lazarus, D. T. Young, in The Giotto Mission-Its Scientific Investigations, ESA-SP1077, eds. R. Reinhard, B. Battrick, p. 129, 1986a.

Balsiger, H., K. Altwegg, F. Buehler, J. Geiss, A. G. Ghielmetti, B. E. Goldstein, R. Goldstein, W. T. Huntress, W.-H. Ip, A. J. Lazarus, A. J. Meier, M. Neugebauer, U. Rettenmund, H. Rosenbauer, R. Schwenn, R. D. Sharp, E. G.Shelley, E. G. Ungstrup, D. T. Young, *Nature, 321,* 330, 1986b.

Coates, A. J., B. Wilken, A. D. Johnstone, K. Jockers, K.-H. Glassmeier, and D. E. Huddleston, Bulk Properties and Velocity Distributions of Water Group Ions at Comet Halley: Giotto Measurements, *J. Geophys. Res., 95,* 10249, 1990.

Cravens, T. E., A magnetohydrodynamical model of the inner coma of Comet Halley, *J. Geophys. Res., 94,* 15025, 1989.

Fuselier, S. A., E. G. Shelley, B. E. Goldstein, R. Goldstein, M. Neugebauer, W.-H. Ip, H. Balsiger, and H. Rème, Observations of Solar Wind Ion Exchange in the Comet Halley Coma, draft manuscript, 1990.

Fuselier, S. A., E. G. Shelley, H. Balsiger, J. Geiss, B. E. Goldstein, R. Goldstein, and W.-H. Ip, Cometary H_2^+ and Solar Wind He^{2+} Dynamics Across the Halley Cometopause, *Geophys. Res. Letts., 15,* 549, 1988.

Glassmeier, K. H., F. M. Neubauer, M. H. Acuña, and F. Mariani, Low-frequency magnetic field fluctuations in comet P/Halley's magnetosheath: Giotto observations, *Astron. Astrophys., 187,* 65, 1987.

Goldstein, B. E., M. Neugebauer, H. Balsiger, J. Drake, S. A. Fuselier, R. Goldstein, W.-H. Ip, U. Rettenmund, H. Rosenbauer, R. Schwenn, and E. G. Shelley, Giotto-IMS observations of ion-flow velocities and temperatures outside the magnetic cavity of comet P/Halley, *Astron. Astrophys., 187,* 174, 1987.

Gringauz, K. I., T. I. Gombosi, M. Tatrallyay, M. I. Verigin, A. P. Remizov, A. K. Richter, I. Apathy, I. Szemerey, A. V. Dyachkov, O. V. Balakina, A. F. Nagy, *Geophys. Res. Letts., 13,* 613, 1986.

Ip, W.-H., On charge exchange effect in the vicinity of the cometopause of Comet Halley, *Astrophys. J., 343,* 946, 1989.

Kettmann, G., W.-H. Ip, H. Balsiger, B. E. Goldstein, A. Meier, H. Rosenbauer, R. Schwenn, and E. G. Shelley, Cometary Ion Flow Variations at Comet P/Halley as Observed by the Giotto IMS Experiment, *Annales Geophysicae, 8,* 229, 1990.

Lämmerzahl, P., D. Krankowsky, R. R. Hodges, U. Stubbemann, J. Wowries, I. Herrwerth, J. J. Berthelier, J. M. Illiano,P. Eberhardt, U. Dolder, W. Schulte, and J. H. Hoffman, Expansion velocity and temperatures of gas and ions measured in the coma of comet P/Halley, *Astron. Astrophys., 187,* 169, 1987.

Neubauer, F. M., K. H. Glassmeier, M. Pohl, J. Raeder, M. H. Acuna, L. F. Burlaga, N. F. Ness, G. Musmann, F. Mariani, Mk. K. Wallis, E. Ungstrup, H. U. Schmidt, First results from the Giotto magnetometer experiment at comet Halley, *Nature, 321,* 352, 1986.

Neubauer, F. M., Giotto magnetic-field results on the boundaries of the pile-up region and the magnetic cavity, *Astron. Astrophys., 187,* 73, 1987.

Neugebauer, M., F. M. Neubauer, H. Balsiger, S. A. Fuselier, B. E. Goldstein, R. Goldstein, F. Mariani, H. Rosenbauer, R. Schwenn, and E. G. Shelley, The variation of protons, alpha particles and the magnetic field across the bow shock of comet Halley, *Geophys. Res. Letts., 14,* 995, 1987.

Neugebauer, M., R. Goldstein, B. E. Goldstein, S. A. Fuselier, H. Balsiger, and W.-H. Ip, Densities and Abundances of Hot Cometary Ions in the Coma of P/Halley, accepted for publication, *Astrophys. J.,* 1990.

Sauer, K., and U. Motschmann, Plasma Boundaries at Comet Halley, preprint, Institut für Kosmosforschung, Berlin, 1989.

Schmidt, H. U., and R. Wegmann, A MHD Model of Cometary Plasma and Comparison with Observations, to appear in the Proceedings of the 1989 Chapman Conference in Guildford, 1990.

Schwenn, R., W.-H. Ip, H. Rosenbauer, H. Balsiger, F. Bühler, R. Goldstein, A. Meier, and E. G. Shelley, Ion temperature and flow profiles in comet P/Halley's close environment, *Astron. Astrophys., 187,* 160, 1987.

Shelley, E. G., S. A. Fuselier, H. Balsiger, J. F. Drake, J. Geiss, B. E. Goldstein, R. Goldstein, W.-H. Ip, A. J. Lazarus, and M. Neugebauer, *Astron. Astrophys., 187,* 304, 1987.

Wegmann, R., H. U. Schmidt, W. F. Huebner, and D. C. Boice, Cometary MHD and Chemistry, *Astron. Astrophys., 187,* 339, 1987.

Yoon, P. H., Kinetic Instability Associated with Spherical Shell Distribution of Cometary Pickup Ions, *Geophys. Res. Letts., 17,* 1033, 1990.

Yoon, P. H., and L. F. Ziebbel, Development of Pitch Angle Anisotropy and Velocity Diffusion of Pickup Ion Shell Distribution by Solar Wind Turbulence, *J. Geophys. Res., 95,* 17085, 1990.

FIGURE CAPTIONS

Fig. 1 The velocity measured by HERS in instrument coordinates. The direction from the comet is downwards (along the vertical axis of the plot). The line at an angle of 15° from the comet direction represents the inner edge of the HERS sensor field of view. The modelling procedure used to estimate the bulk velocities can not compensate for velocity shells of cold pick-up ions that are entirely within the unobserved cone. Thus, the estimates do not approach the ram velocity (i.e., the vertical axis) as the comet is approached. The observation points are indicated by + symbols on the curve and are average values centered at the times (UT) given in the box on the plot. The first datum (23:13:40) is the leftmost point in the plot.

Fig. 2. Plasma parameters obtained by the HERS for the period 19:00 UT to 24:00 UT. The solid lines are proton data, the dashed lines are alpha particle data, and the dotted lines are water group data. The speed (km/sec) in a comet centered frame is shown in the upper panel, the next panel shows number density (cm^{-3}, the scale on the left is for protons and for alpha particles multiplied by 10, the scale on the right is for the water group ions), the next panel shows log temperature (K), and the lowest panel shows pressure ($dynes/cm^2$). The ion temperature does not include contributions from particles in velocity shells with radii greater than 100 km/sec.

Fig. 3. Contours of common logarithm of phase space density in units of $cm^{-6}sec^3$ of mass 17 ions for a 5 minute averaging period centered at 23:27:39 UT. The cross is at the location where new pick-up ions are created.

Fig. 4. Phase space densities (arbitrary units) of spherical velocity shells with the bottom line being the earliest data and the top line being the latest. The times shown on the figure are UT. The vertical arrows indicate the average pick up velocity during the period of measurement.

Fig. 5. Average phase space densities (units of $cm^{-6}sec^3$) in velocity space of spherical shells 10 km/sec in thickness. The data are similar to those shown in Fig. 4 except that the velocity space intervals are 10 km/sec, and the time centers of the averaging intervals are different. The format allows numerical values to be ascertained without ambiguity.

Fig. 6. A comparison in aberrated HSE coordinates between the large scale flow direction observed by the IMS (HERS and HIS) and the MHD calculations of Wegmann *et al.* (1987, see their Fig. 3b). The units of the axes are 10^6 km. See text for interpretation of magnitude of vectors.

Fig. 7. A comparison in aberrated HSE coordinates between the large scale flow direction observed by the HIS and the MHD calculations of Wegmann *et al.* (1987, see their Fig. 4b). The units of the axes are 10^4 km. The vertical line in the lower center of the figure is the length of a 10 km sec velocity vector.

Fig. 8. A comparison between flow parameters measured by the IMS and the MHD calculations of Schmidt and Wegmann (1990). N, v, and T_i, are the number density, the velocity, and the ion temperature of the calculation (medium thickness lines), N_W, V_W, and T_W, are the number density, velocity, and temperature of water group ions as measured by the HERS sensor (heaviest lines), and (thinnest lines) N_p is proton number density, V_a is the velocity of the alpha particles, V_h and T_h are the velocity and temperature of the water group ions as measured by the HIS sensor.

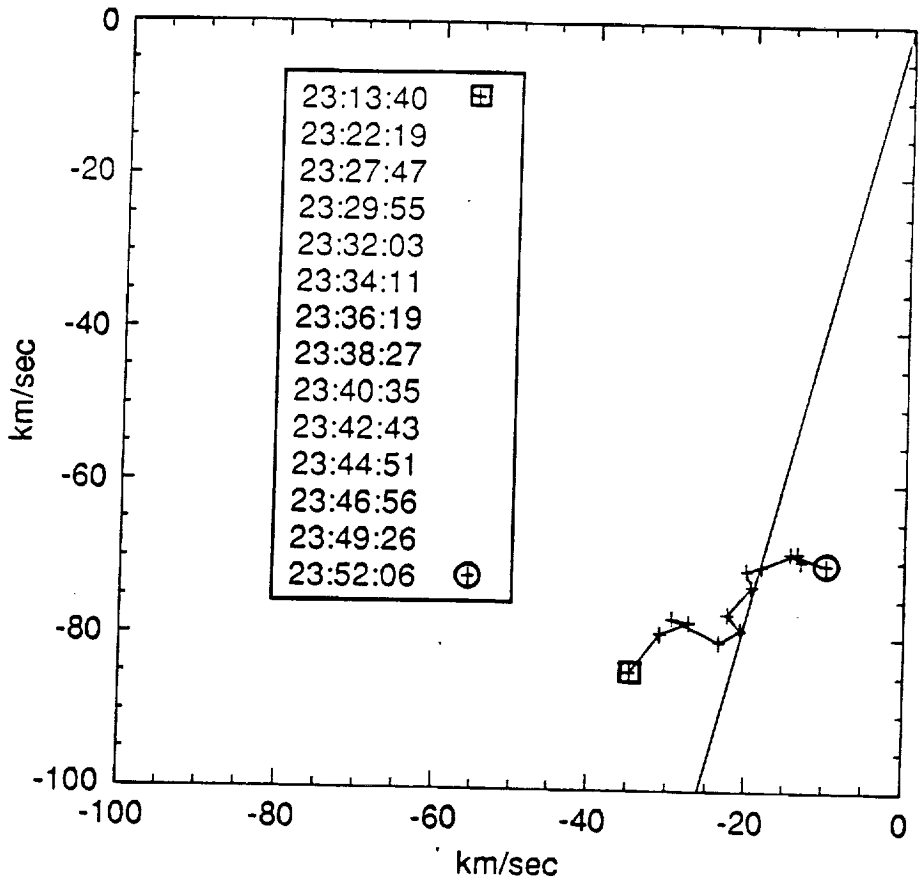

23:13:40
23:22:19
23:27:47
23:29:55
23:32:03
23:34:11
23:36:19
23:38:27
23:40:35
23:42:43
23:44:51
23:46:56
23:49:26
23:52:06
0
-20
-40
-60
-80
-100
-100
-80
-60
-40
-20
0
km/sec
km/sec

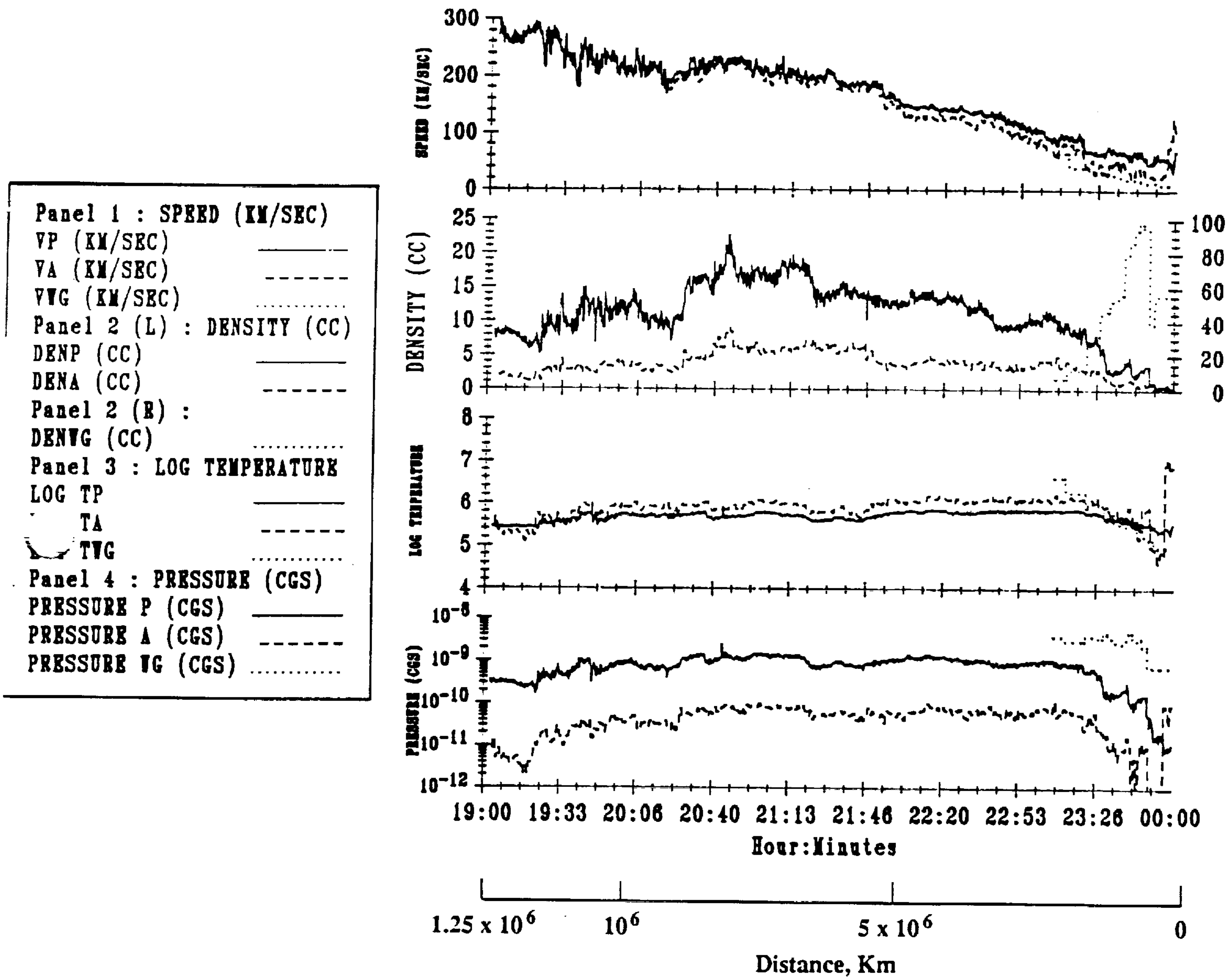

Panel 1 : SPEED (KM/SEC)
VP (KM/SEC)
VA (KM/SEC)
VWG (KM/SEC)
Panel 2 (L) : DENSITY (CC)
DENP (CC)
DENA (CC)
Panel 2 (R) :
DENWG (CC)
Panel 3 : LOG TEMPERATURE
LOG TP
TA
TWG
Panel 4 : PRESSURE (CGS)
PRESSURE P (CGS)
PRESSURE A (CGS)
PRESSURE WG (CGS)
SPEED (KM/SEC)
300
200
100
0
DENSITY (CC)
25
20
15
10
5
0
100
80
60
40
20
0
LOG TEMPERATURE
8
7
6
5
4
PRESSURE (CGS)
10^{-8}
10^{-9}
10^{-10}
10^{-11}
10^{-12}
19:00 19:33 20:06 20:40 21:13 21:46 22:20 22:53 23:26 00:00
Hour:Minutes
1.25×10^6
10^6
5×10^6
0
Distance, Km

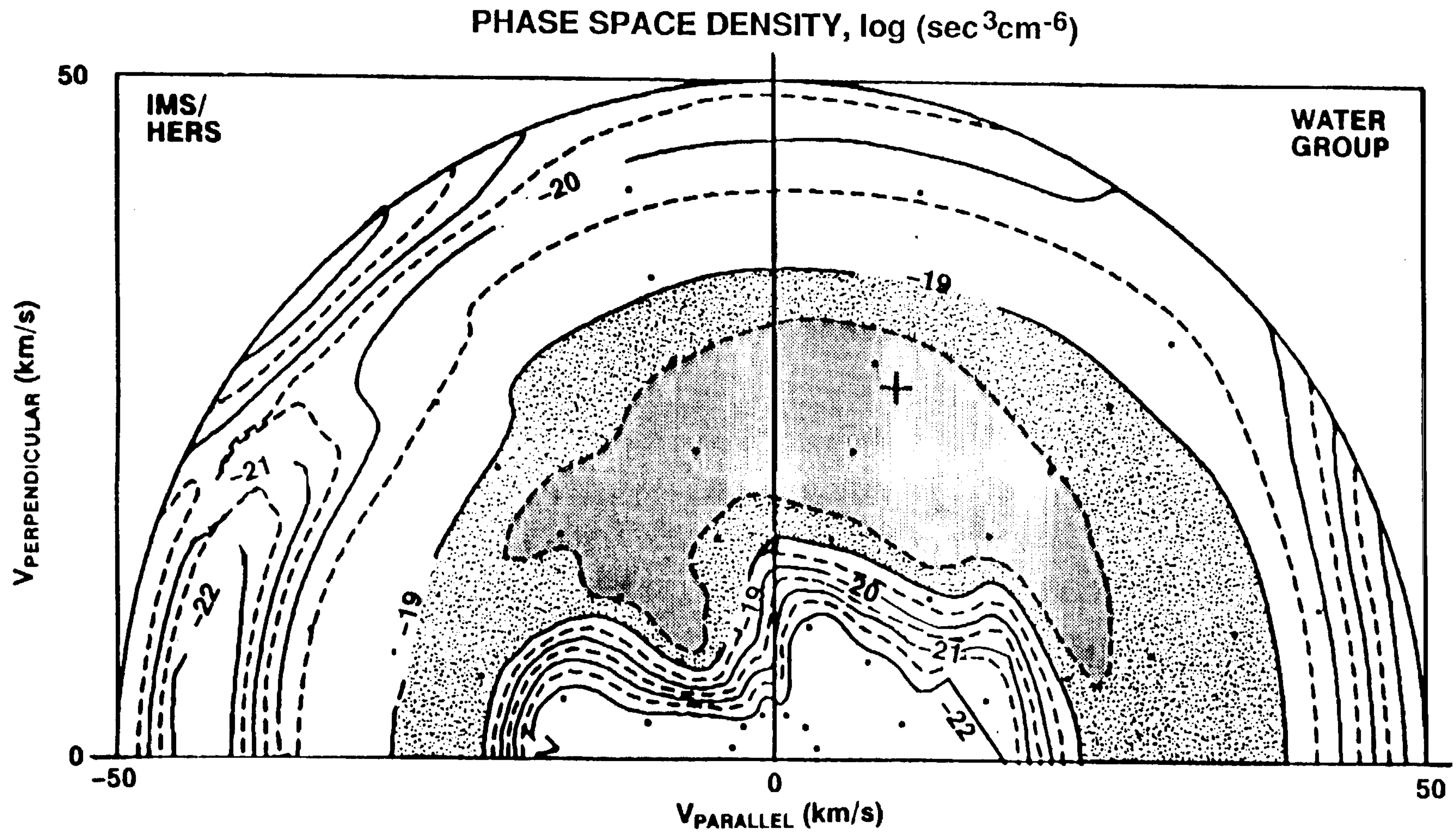
PHASE SPACE DENSITY, log (sec^{3}cm^{-6})
IMS/
HERS
WATER
GROUP
-20
-19
-21
-22
-19
-19
-20
-21
-22
50
0
-50
0
50
$V_{PERPENDICULAR}$ (km/s)
$V_{PARALLEL}$ (km/s)

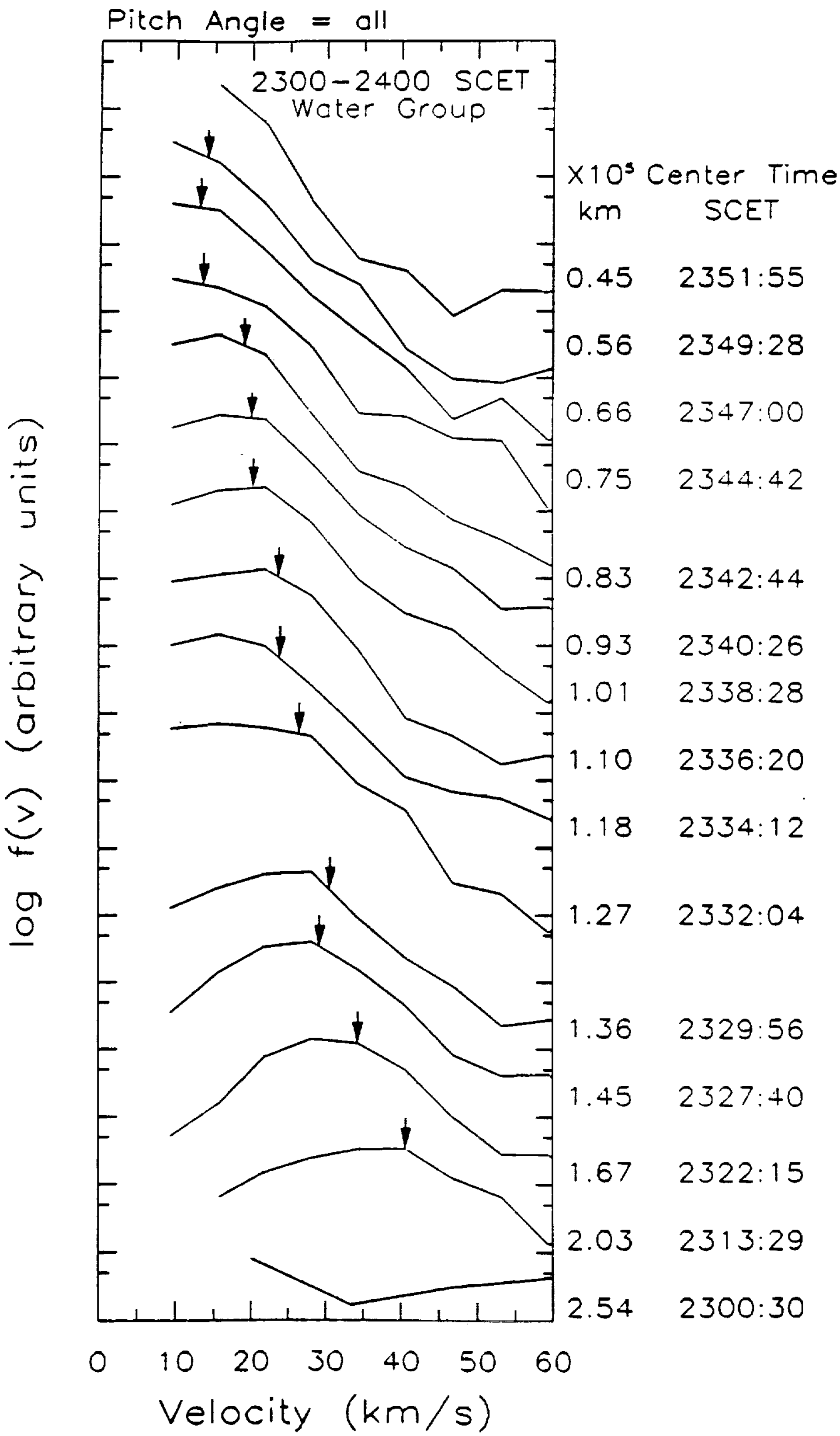

Pitch Angle = all
2300-2400 SCET
Water Group
X10⁵ km
Center Time SCET
0.45 2351:55
0.56 2349:28
0.66 2347:00
0.75 2344:42
0.83 2342:44
0.93 2340:26
1.01 2338:28
1.10 2336:20
1.18 2334:12
1.27 2332:04
1.36 2329:56
1.45 2327:40
1.67 2322:15
2.03 2313:29
2.54 2300:30
log f(v) (arbitrary units)
0 10 20 30 40 50 60
Velocity (km/s)

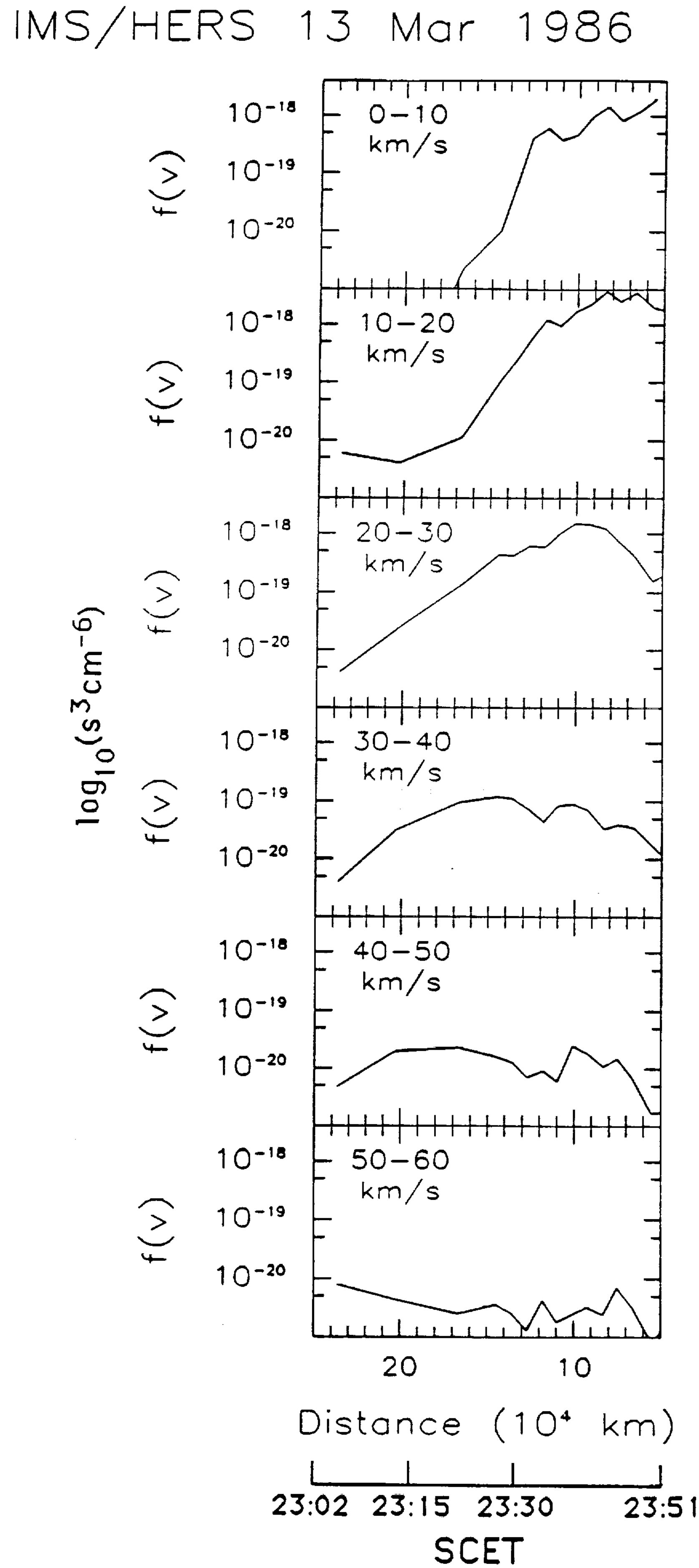
IMS/HERS 13 Mar 1986
0–10 km/s
10–20 km/s
20–30 km/s
30–40 km/s
40–50 km/s
50–60 km/s
f(v)
10^{-18}
10^{-19}
10^{-20}
$\log_{10}(s^3cm^{-6})$
20
10
Distance (10^4 km)
23:02 23:15 23:30 23:51
SCET

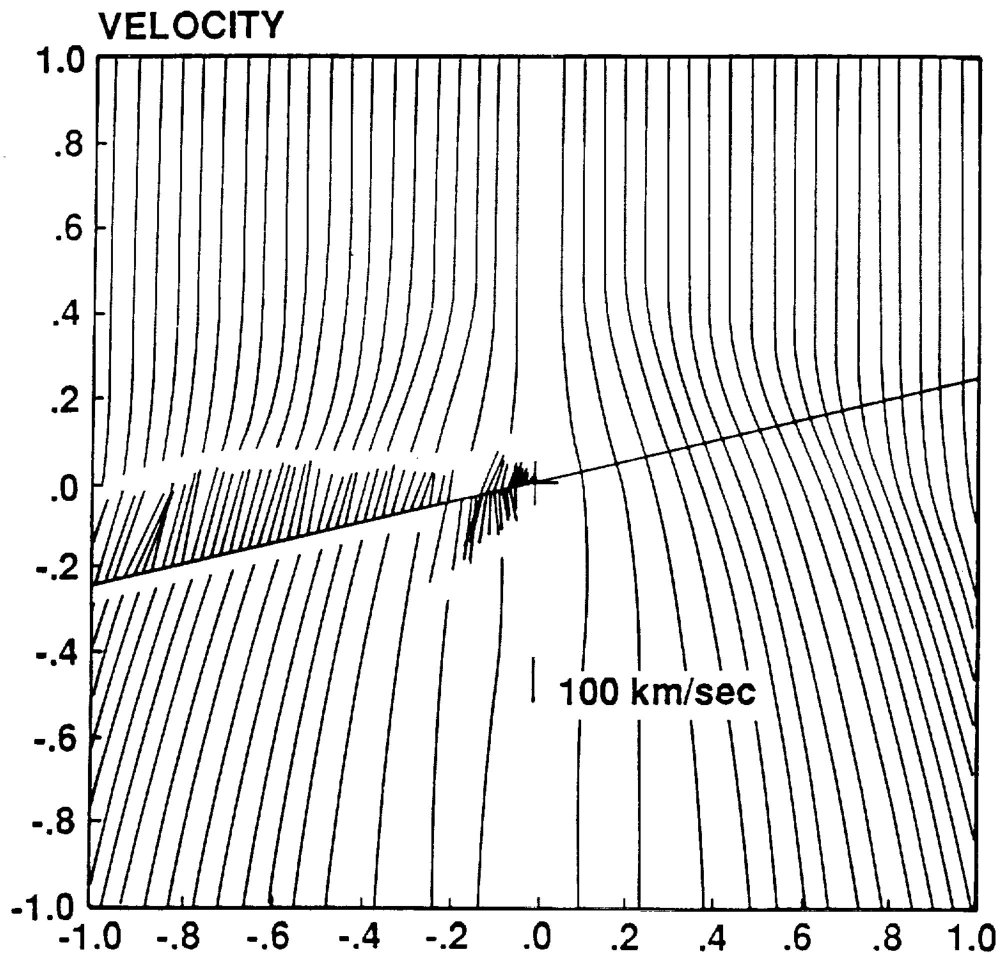

VELOCITY
1.0
.8
.6
.4
.2
.0
-.2
-.4
-.6
-.8
-1.0
100 km/sec
-1.0
-.8
-.6
-.4
-.2
.0
.2
.4
.6
.8
1.0

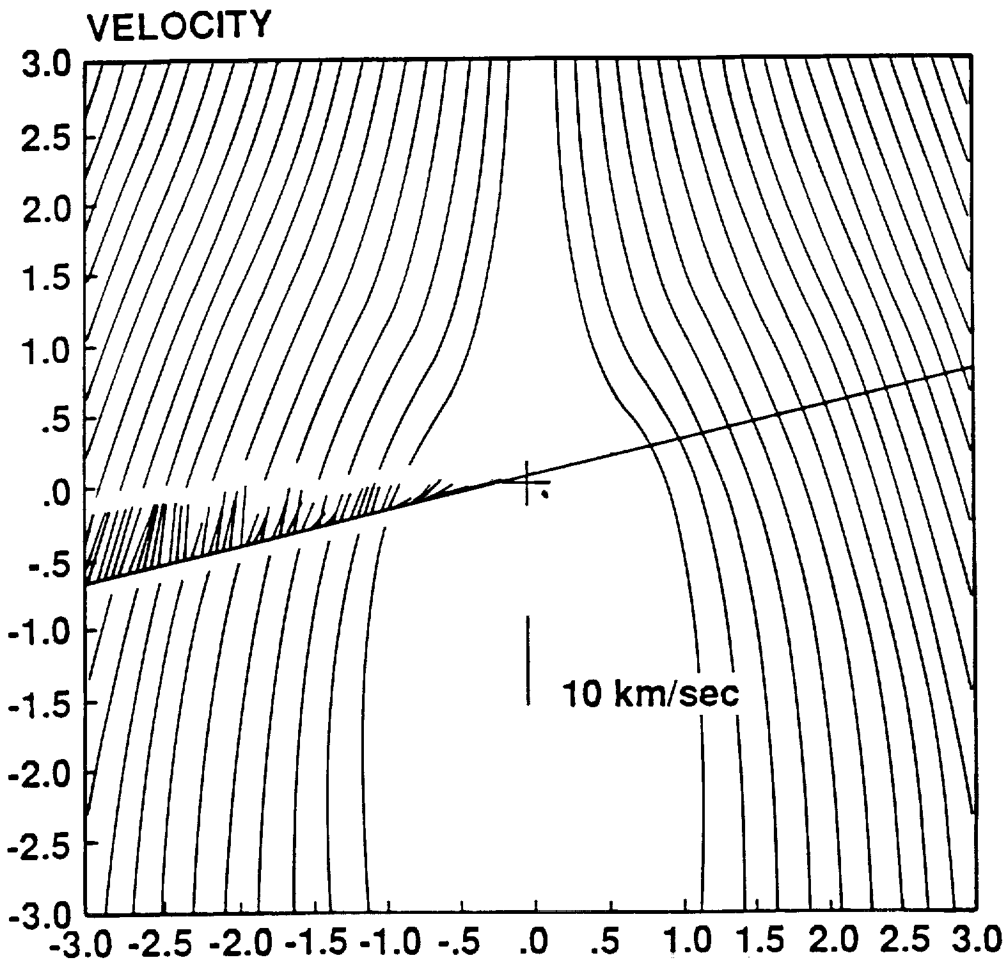
VELOCITY
3.0
2.5
2.0
1.5
1.0
.5
.0
-.5
-1.0
-1.5
-2.0
-2.5
-3.0
10 km/sec
-3.0 -2.5 -2.0 -1.5 -1.0 -.5 .0 .5 1.0 1.5 2.0 2.5 3.0

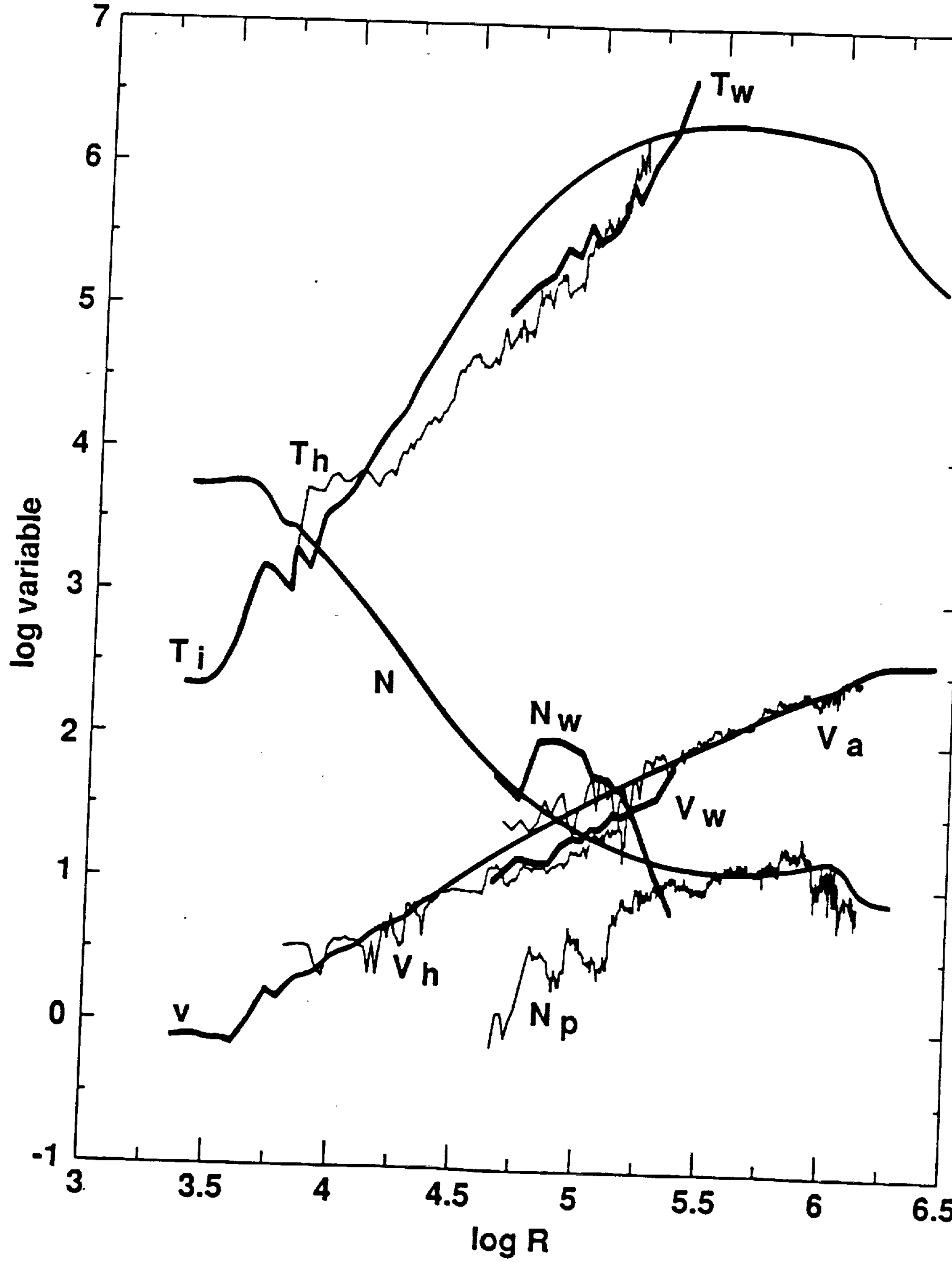

7
6
5
4
3
2
1
0
-1
log variable
3
3.5
4
4.5
5
5.5
6
6.5
log R
Tw
Th
Ti
N
Nw
Va
Vw
Vh
v
Np